SECOND EUROPEAN CONFERENCE ON EARTHQUAKE ENGINEERING
AND SEISMOLOGY, ISTANBUL AUG. 25-29, 2014

MICRO-MODELING OF TESTED FRAMED-WALL WITH OPENINGS

Davorin PENAVA[1], Vladimir SIGMUND[2] and Ivica KOŽAR[3]

ABSTRACT

This paper uses micro modelling as a substitute for missing tests of reinforced concrete frames with openings but one cannot just use material data resulting from simple tests performed on a single material. Material behaviour in composite structures like reinforced concrete frames depends on their interaction that cannot be analysed in single material tests so the model parameters have to be calibrated on tests on structures. The model is then used to extrapolate results on other cases of interest but without any guarantee that the obtained results would be safe. In this paper we report on difficulties and obstacles found in this process. The analysed cases comprise the window and door openings of medium size, centrically or eccentrically positioned within unreinforced masonry infill made of clay hollow masonry units and general purpose mortar. We discuss the physical meaning of material properties used in the model and limitations of the model extrapolation.

INTRODUCTION

Structural unreinforced infill wall within reinforced concrete frame or as together framed-wall, with or without unconfined or confined openings, are difficult to model. This is primarily because of the lack of knowledge about their interaction, complex failure mechanisms and the vast material properties needed, yet impossible to include (or known) them all.

Methodology called micro-modelling works by defining each element i.e. brick and joint individually, compared to equivalent diagonal strut i.e. macro-model which replaces the complete infill wall (Stafford-Smith, 1966). The need for material data exceeds standard properties that can be determined by simple tests thus the scientist (rather than engineer) must seek for theoretical sources to complete his task. Another, but not less important, is the computational demand which limits this type of analysis on a frame or two. Even if previous is arranged one cannot just proceed with the analysis since results will surely not be adequate i.e. not real. This is primary the reason for the usage of this method only and if only tests are provided first.

In this paper we report on the encountered problems with non-linear finite element analysis of previously tested framed-walls with window or door opening, centrically or eccentrically positioned. The idea was to show the differences in results between two approaches. The first was by taking simplest (naive) approach of input the material properties and obtaining results and the second is by so-called calibration. We found that certain effects that are not usually taken into account e.g. inclination of the mortar in masonry unit hollows can influence the results significantly. The modelling of bedjoint after the initial shear strength was reached was crucial for the calibration. Framed-wall's cyclic response description using the micro-modelling approach demands good experimental background of the whole model and its constituents especially in nonlinear range (initial values were proven not to be enough).

[1] Assistant Professor, Josip Juraj Strossmayer University of Osijek, Osijek, dpenava@gfos.hr
[2] Full Professor, Josip Juraj Strossmayer University of Osijek, Osijek, sigmund@gfos.hr
[3] Full Professor, University of Rijeka, Rijeka, ivicak@gradri.hr

MATERIALS AND METHODOLOGY

The background of the investigation presented is the tests that were carried on six specimens of reinforced-concrete frames of which five were with infill wall and one without, produced in a scale 1:2,5, as described in (Sigmund & Penava, 2014). Within the masonry infill an unconfined opening representing a door or window, centrically or eccentrically positioned, of medium size $A_o/A_i<0.15$ was executed (see Table 1.). Material property values in Table 2. present single average value of all specimens for the purpose of unification. They also represent mean values as stated in EC8.

Table 1. Classification and description of the specimens

Specimen	Specimen sketch	Opening type, area and dimensions	Opening position
I/1	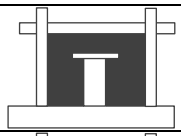	Door l_o/h_o=0.35/0.90 m A_o=0.32 m^2 A_o/A_i=0,14	Centric e_o= l_i/2 =0.90 m
I/2	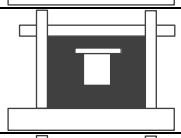	Window l_o/h_o=50.0/60.0 cm A_o=0.30 m^2 A_o/A_i=0,13	Centric e_o= l_i/2 =0.90 m P=0.40 m
I/3	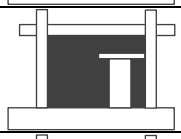	Door l_o/h_o=0.35/0.90 m A_o=0.32 m^2 A_o/A_i=0,14	Eccentric e$_o$=h_i/5+l_o/2=0.44 m
I/4	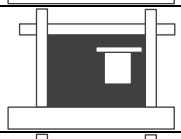	Window l_o/h_o=50.0/60.0 cm A_o=0.30 m^2 A_o/A_i=0,13	Eccentric e_o=h_i/5+l_o/2=0.44 m P=0.40 m
III/1	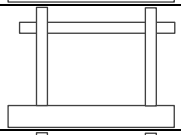	-	-
III/2	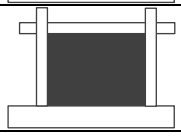	-	-

A_o=h_o*l_o is area of an opening, A_i=h_i*l_i is area of a masonry infill, l_o is opening length, h_o is opening height, h_i=1.3 m is infill wall height, l_i=1.8 m is infill wall length, e_o is opening eccentricity, t_i=0.12 m is infill wall thickness, P is parapet wall

Table 2. Mechanical properties of materials used obtained through tests

Material	Symbol	Value	Units	Meaning
Concrete of the Frame	f_{cm}	=58	N/mm^2	mean value of cylinder compressive strength
	E_{cm0}	=41000	N/mm^2	mean initial modulus of elasticity
Concrete of the Lintel	f_{cm}	=26	N/mm^2	mean value of cylinder compressive strength
Clay Hollow Masonry Unit	f_{mubm}	=17,5	N/mm^2	mean compressive strength of the masonry unit
	E_{mu0bm} /E_{muh0m}	=5650/850	N/mm^2	mean initial modulus of elasticity of the masonry unit
Steel Reinforcement	f_{ym}/f_{um}	=550/650	N/mm^2	mean yield and mean ultimate strength of reinforcing steel
Masonry Unit and Mortar Joint Interface	f_{v0m}	=0,35	N/mm^2	mean initial shear strength of a masonry
	f_{tm}	=0,2	N/mm^2	mean initial tensile strength of a masonry
	μ_m	=0,25	-	friction coefficient

Indices b and h designate reference to the bedjoint (vertical direction) and the headjoint (horizontal direction) respectively

Reinforced-concrete frames were executed in compliance with EC2 and EC8 as medium ductility frames (DCM) as shown in Fig.1.

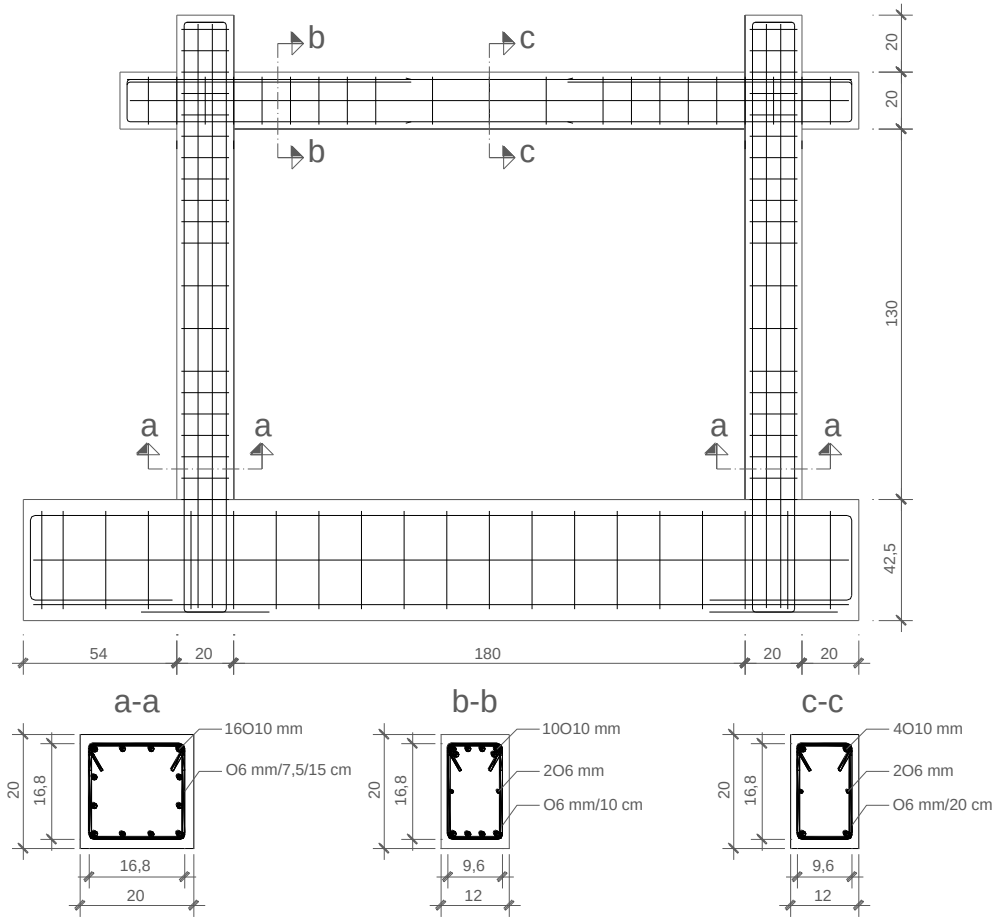

Figure 1. Reinforcing details of framed-wall specimens (Note: dimensions in cm)

Specimens were tested under constant vertical (axial in columns) and in-plane lateral (shear) repeated cyclic loading with force control, as to be closer to earthquake action (earthquake doesn't causes prescribed displacements). The test setup scheme is given in Fig.2. The load application scheme is given next.

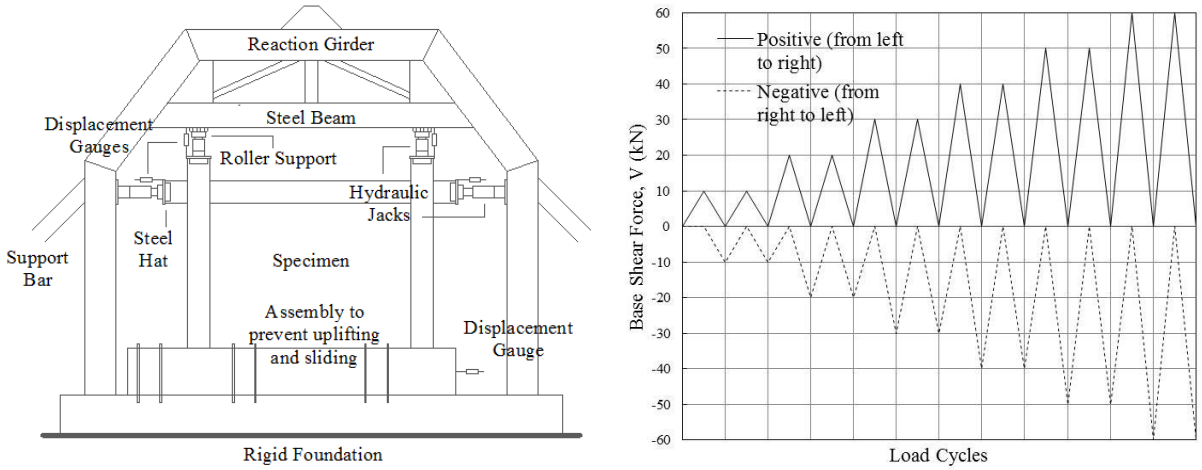

Figure 2. Test setup (left) and load application scheme (right)

The models of tested specimens were created as simplified micro-models (brick by brick) in the nonlinear finite element analysis software ATENA 2D ver. 4.3.1.0, due to possession of material models adequate for reinforced-concrete and masonry infill simulation, especially quasi brittle behaviour of clay masonry units. Simplified designates separate definition of masonry units and mortar but without mortar thickness (zero thickness). The material data necessary for the constitutive models not determined through tests and were adopted from theoretical sources e.g. Kranzler, 2008 & Saneinejad, 1990, as given in Table 3. Stated are only the values that were modified with respect their prescribed values given in Červenka, et al., 2012. For each material (element) adopted were the appropriate constitutive law (finite element type mesh density). Special care was taken for the bedjoints since they made a crucial difference in analysis. We marked these cases as 1, 2 and 3.

Concrete of the frame and of the lintel was modelled using the 3D Non Linear Cementitious 2 material model. It is a fracture-plastic model that combines constitutive models for tensile (fracturing) and compressive (plastic) behaviour. The fracture model is based on the classical orthotropic smeared crack formulation and crack band model. It employs Rankine failure criterion and exponential softening. For it, the rotated crack model was adopted because compared to fixed model enabled stability of calculations. Aggregate interlock in shear was also considered. The hardening/softening plasticity model is based on Menétrey-Willam failure surface. Detail description of the constitutive model can be found in ATENA Program Documentation. Compared to other models available in software, chosen model possesses the ability of describing the fat unloading curve and the inclusion of the tension stiffening, which was necessary for proper representation of cyclic response.

Clay hollow masonry units were modelled using SBeta concrete constitutive model due to ability to adequately represent the quasi-brittle behaviour. It follows also an orthotropic smeared approach. Nonlinear behaviour in compression (including hardening and softening) and linear in tension is governed by equivalent uniaxial stress-strain law and biaxial stress failure criterion of concrete (see Fig.3.).

Table 3. Mechanical properties of materials used taken from theoretical sources

Material		Symbol	Value	Units	Meaning
Concrete of the Frame		f_{ctm}	=4	N/mm^2	mean value of axial tensile strength
		v_c	=0.2	-	Poisson's ratio
		G_f	=0.12	N/mm	specific fracture energy
		s_{max}	=125	mm	cracks pacing
		c_{ts}	=0.4	-	tension stiffening coefficient
		$f_{cm.lim}$	=0.1	-	coefficient for reduction of compressive strength due to cracks
Clay Hollow Masonry Unit		ν_{mub}	=0,1	-	Poisson's ratio
		G_{mub0}/ G_{muh0}	=2570/390	N/mm^2	initial modulus of shear of the masonry unit
Masonry Unit and Mortar Joint Interface	Case 1, 2 & 3	K_{nnb}	$=E_{mu0bm}/t_{mb}$=565	N/mm^3	normal stiffness of the masonry unit and mortar bedjoint interface
		K_{ttb}	$=G_{mu0bm}/t_{mb}$=257	N/mm^3	tangential stiffness of the masonry unit and mortar bedjoint interface
		K_{nnh}	$=E_{mh0hm}/t_{mh}$=85	N/mm^3	normal stiffness of the masonry unit and mortar headjoint interface
		K_{tth}	$=G_{mu0hm}/t_{mh}$=39	N/mm^3	tangential stiffness of the masonry unit and mortar headjoint interface
	Case 2	f_{v0m}	=0,7	N/mm^2	mean initial shear strength of a masonry
		f_{tm}	=0,45	N/mm^2	mean initial tensile strength of a masonry
		μ_m	=0,8	-	friction coefficient at the mortar joint and the masonry unit interface
	Case 3	f_{vltbm}	$=0.065f_{mub}$=1.14	N/mm^2	mean shear strength limiting value in accordance with EC6

t_m=10 mm is thickness of the mortar joint; indices b and h designate reference to bedjoint and headjoint respectively

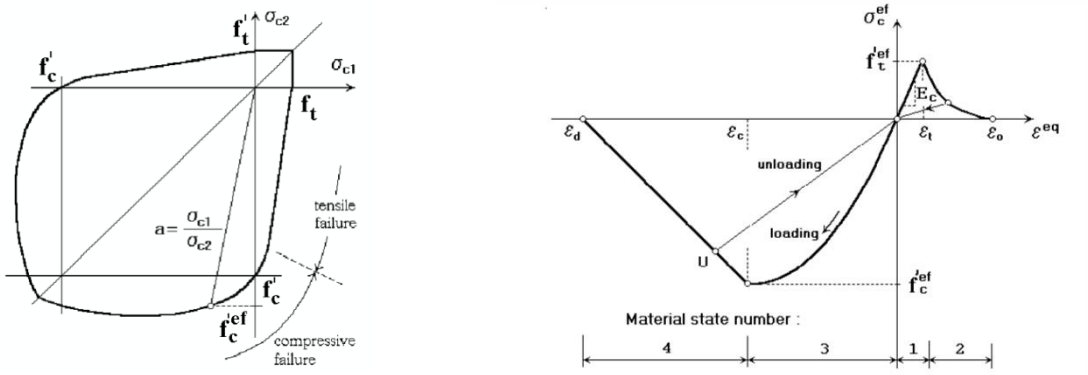

Figure 3. Biaxial failure function (left) and uniaxial stress-strain law (right) for SBeta constitutive model

In tension after cracking an exponential crack opening law is adopted together with rotated crack model. In compression post peak the end point of the softening curve is defined by means of the plastic displacement. The model can produce crack but not discrete i.e. the unit cannot break. The clay hollow masonry units were modelled as solid, using the properties of material perpendicular to bedjoints (vertical direction). Model doesn't allow taking the orthotropic properties that exist in different directions due to units hollows (see Table 1). The lack of modelling the orthotropic properties was compensated by defining mortar bedjoints and headjoints differently and by using interface normal and tangential stiffness.

Mortar headjoints and bedjoints were modelled using the Interface material model (see Fig.4.). It is a model based on Mohr-Coulomb criterion with tension cut off. The model is elastic in compression. Three approaches i.e. cases for the modelling of mortar joints have been set. In the first used were the material properties obtained from tests. In the second case instead of tested, the theoretical values from literature sources were introduced, while in the third case the values from first case i.e. original tests. The difference in-between the first and the third case is the user defined function (shear stress-displacement) for softening or hardening after the failure of the initial shear strength for the bedjoints. This had to be done due to inclination of mortar in hollows of masonry units, as occurred in tests. The highest value of the function was defined as the failure of the unit (see Table 2.) i.e. by using the limit value for shear from EC6. Corresponding displacements have been established through trial and error process (see Fig.5.). The tensile strength is assumed as immediate loss as soon as the strength value was reached i.e. the default value was not modified.

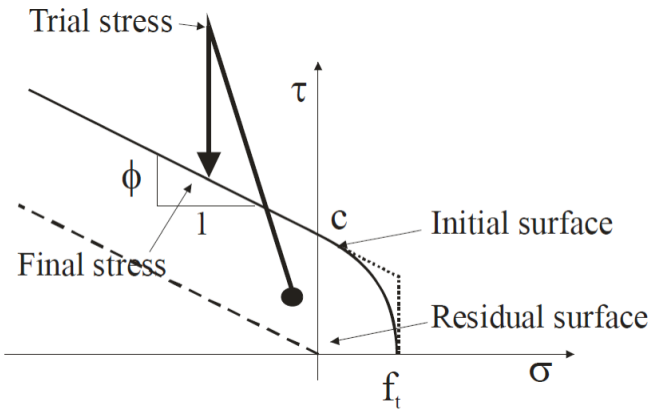

Figure 4. Mohr-Coulomb criterion for Interface material model

In all cases properties obtained for bedjoints were assigned equal for the bedjoints and headjoints. On the other hand, also in all cases, normal and also tangential stiffness was different. This is the result of their estimation on the basis of initial modulus of elasticity of neighbouring elements i.e. masonry units. At the contact with the concrete frame or lintel the joint stiffness was assumed as in other places in the infill wall. Due to zero thickness of the interface material model masonry units were expanded to supplement it.

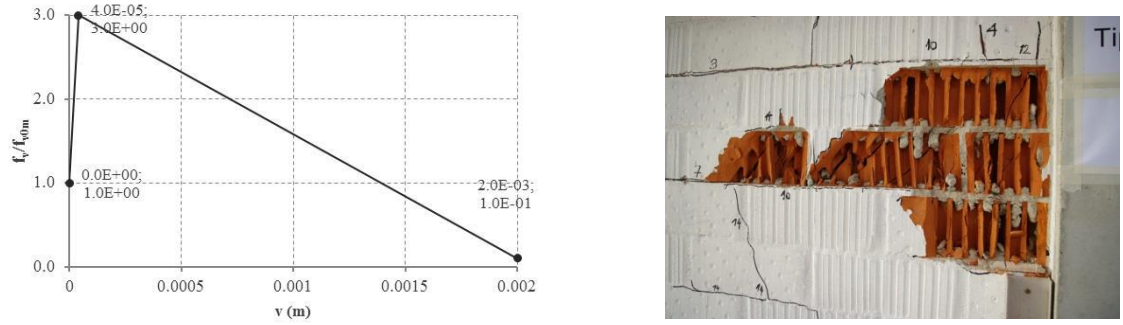

Figure 5. User defined function for shear (left) and failed masonry unit with inclined mortar (right)

Longitudinal and transversal steel reinforcement was modelled using the Menegoto-Pinto cyclic reinforcement material model defined by bilinear with hardening stress-strain law. It was adopted that the reinforcement is active in compression and that perfect bond between the reinforcement and the concrete exists. In order to compensate the lack of bending and shear stiffness (dowel action) for the discrete reinforcement bars in longitudinal direction, transversal bars were supplied with additional area (Pryl & Červenka, 2013). This area was equal to area of longitudinal reinforcement at observed plane. Also, the transversal bars at the beam and column ends had to be moved from the exact crossing line in between the different structural parts. This was especially at the column ends to prevent extensive concrete cracking (softening) in that region. It was observed on the numerical model that at higher cycles of loading that the crack influence becomes higher than in reality.

Steel pad was modelled using the Plane Stress Elastic Isotropic constitutive law. Its idea was to take the point loads and transmit them equally to the beam and column ends, which would otherwise cause inappropriate response. It was also used as the place where the applied loads and observed displacements were monitored.

Frame, lintel, steel pad and masonry units were modelled using plane quadrilateral and triangular finite elements, CCIsoQuad and CCIsoTriangle, respectively. Longitudinal and transversal reinforcement was modelled using the discrete bars with the help of CCIsoTruss elements. Interface was modelled using the nonlinear geometry CcIsoGap elements. The size of the elements set to 5 cm was proven to be adequate for accuracy and time of calculations. The elements are shown in Fig.6.

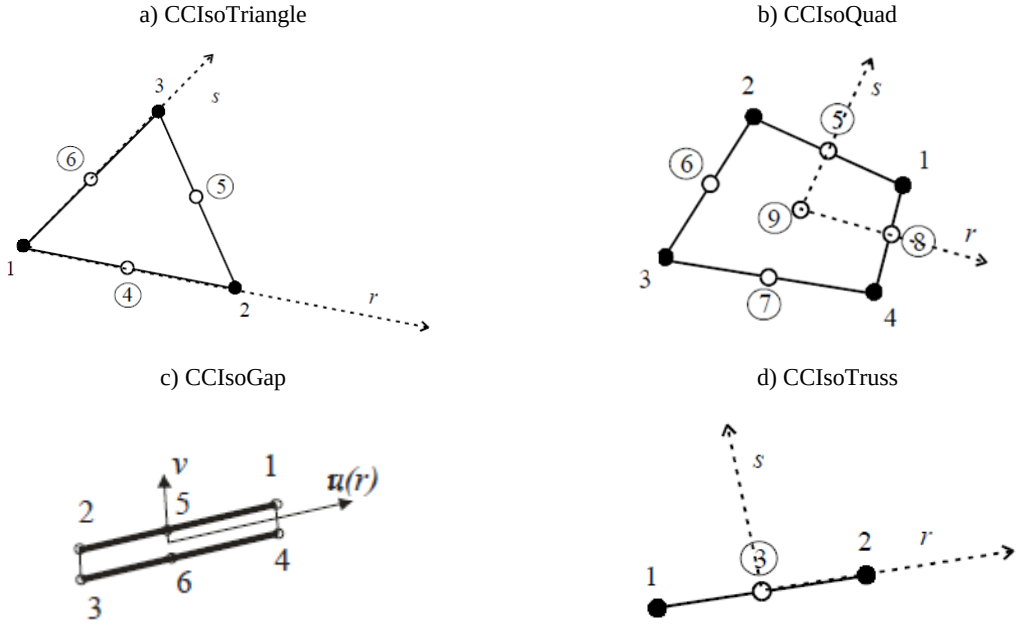

Figure 6. Geometry of the finite elements used

Boundary conditions of the model were built to match those from tests, as shown in Fig.2. Fixed supports were added to the bottom line of foundation beam while sliding supports were placed on column tops. Additionally, support was assigned to the beam left and right end to prevent vertical movement. The last two were set to be active after vertical constant load on columns tops was applied. In horizontal direction load was applied in cycles according to Fig.2 at left and right beam end i.e. positive and negative direction. Both loads were applied as point loads on steel pads.

For the solution of the nonlinear equations the Full Newton-Rapshon method was employed because of the loading and response characteristics of tests specimen.

CALCULATIONS AND RESULTS

The calculations were carried out in full accordance with the tests and description above to obtain equal response. For the control of calculations primary (envelope) curves and crack (damage) pattern as visual identification were used (see Fig.7,8 and 10.). The graphs show relation in-between the average displacement d (mm) and applied base shear force V (kN) on primary axes, and drift ($d_r=d/(h_i+d_b/2)$ in % and base shear ratio (ratio of shear towards total axial loading) on secondary axes.

The frame without infill wall was calibrated first to eliminate one unknown from the framed-wall system (establish a foothold). Then the analyses on frame with complete infill wall were employed. In this step three approaches were exercised with the difference in the definition of mortar joints as described earlier. These were necessary to obtain the satisfactory coincidence with the test results. After obtaining good correlation with the tests (cases 2 and 3) the same material data were used for the infill wall with opening cases. After unsuccessful attempt using the case 2 approaches, the case 3, provided unique solution for all the specimens. Results are given separately for each case previously described and compared to the ones from corresponding test.

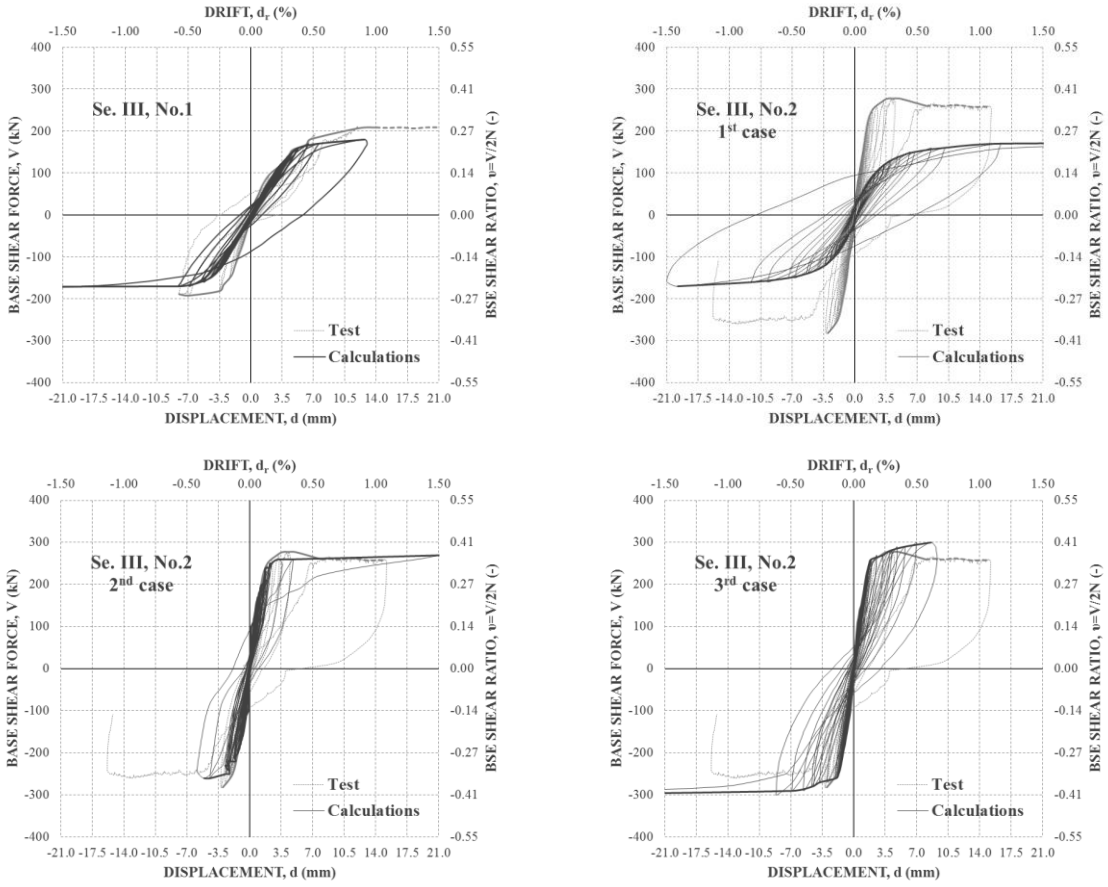

Figure 7. Comparison of response obtained by tests and calculations for frame without and with infill wall

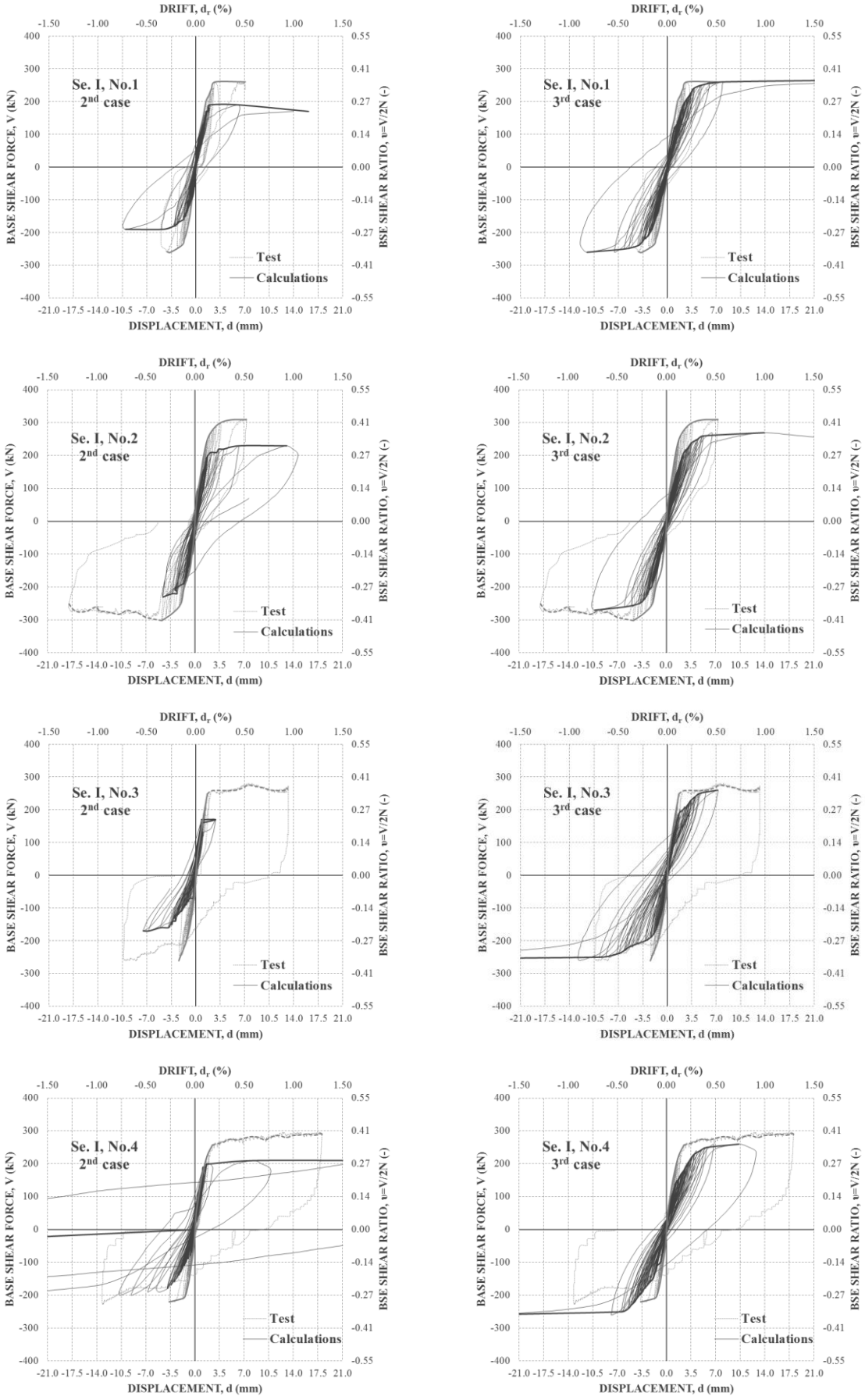

Figure 8. Comparison of response obtained by tests and calculations for frame without and with infill wall

In Fig.9. shown are the cracked specimens at the breaking stage of the infill wall. The finite element mesh is also visible. The frame without infill wall is not shown, since cracks obtained are coincidental with other specimens i.e. bending tensile cracks.

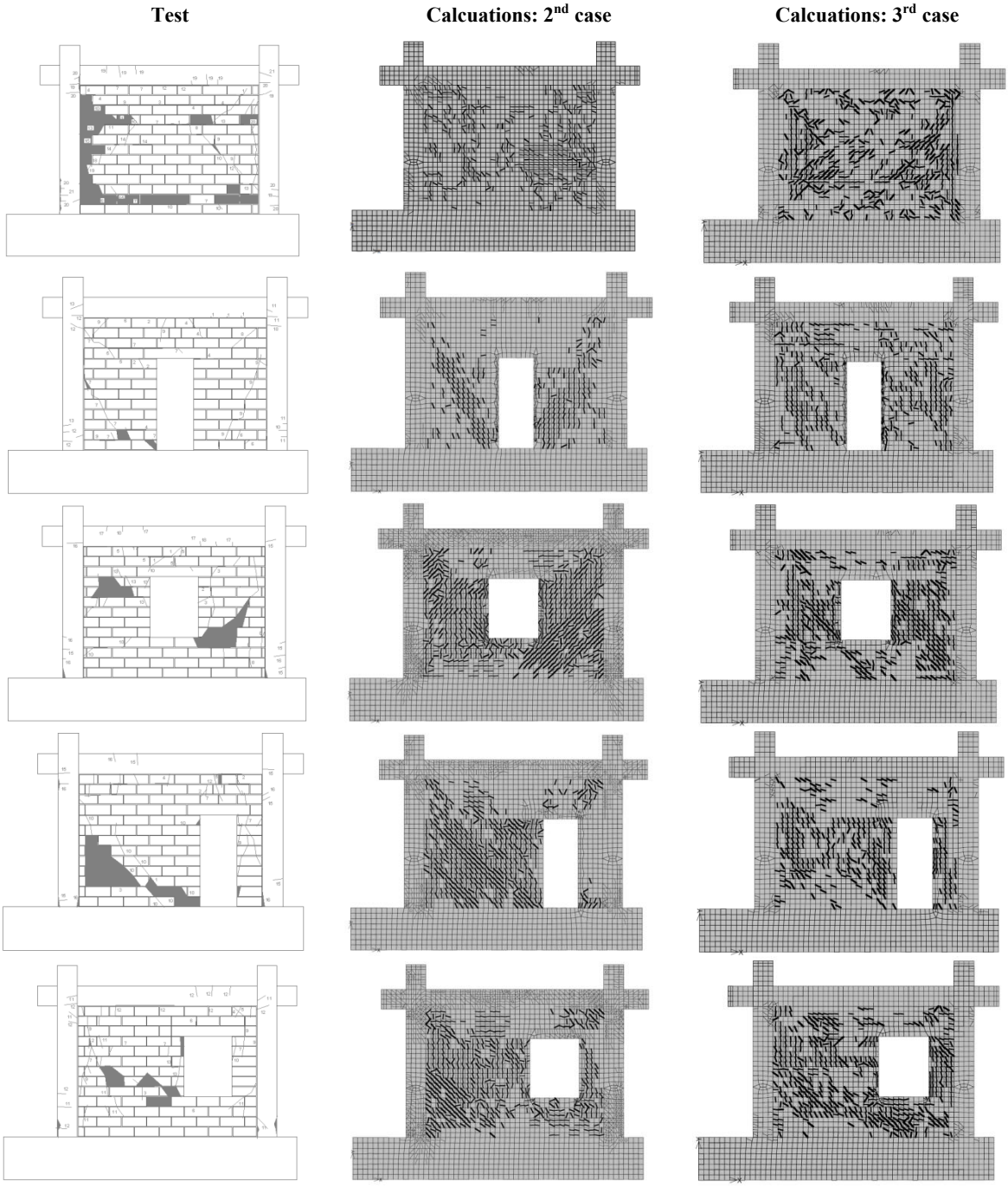

Figure 9. Cracks at break point of the infill wall

In Tables 4. and 5., shown are the differences in-between tests and calculations in terms of secant stiffness K (kN/mm) and energy dissipation capacity E (kNmm^2).

The secant stiffness was calculated as base shear force divided with corresponding displacement at four characteristic drift points. These refer to slight (d_r≈0,10%), medium (d_r≈0,25%), heavy (d_r≈0,50%) and pre-collapse damage states (d_r≈1,00%), as described in Sigmund & Penava, 2014.

Table 4. Correlation in-between test and calculations in terms of secant stiffness K (kN/mm) at characteristic drifts

Spec.	d_r (%)	Positive side					Negative side				
		Test	Calc. 2nd case	Calc. 3nd case	Diff. (%)		Test	Calc. 2nd case	Calc. 3nd case	Diff. (%)	
					2nd/test	3rd/test				2nd/test	3rd/test
I/1	0.10	137	104	95	24%	30%	-145	-108	-105	26%	28%
	0.20	95	53	74	44%	23%	-88	-59	-77	33%	13%
	0.50	33	23	33	30%	0%	-26	-26	-38	0%	-46%
	1.00	-	11	6	-	-	-17	-	-23	-	-33%
I/2	0.10	163	109	100	33%	39%	-150	-126	-107	16%	29%
	0.20	103	60	75	42%	27%	-87	-79	-78	9%	10%
	0.50	42	23	44	45%	-4%	-35	-	-44	-	-26%
	1.00	-	12	19	-	-	-22	-	-	-	-
I/3	0.10	160	164	121	-3%	24%	-131	-61	-112	53%	14%
	0.20	93	60	77	35%	17%	-100	-46	-63	54%	37%
	0.50	37	-	36	-	2%	-40	-21	-34	48%	16%
	1.00	20	-	-	-	-	-18	-	-24	-	-34%
I/4	0.10	142	124	95	13%	33%	-150	-51	-83	66%	45%
	0.20	93	72	68	23%	27%	-96	-51	-61	47%	36%
	0.50	40	25	44	38%	-9%	-47	-25	-39	47%	17%
	1.00	19	17	25	11%	-33%	-	-12	-28	-	-
III/1	0.10	45	42		7%		-60	-42		30%	
	0.20	34	37		-9%		-48	-38		21%	
	0.50	22	23		-3%		-22	-28		-29%	
	1.00	12	14		-18%		-16	-21		-	
III/2	0.10	151	147	162	3%	-7%	-151	-151	-163	0%	-8%
	0.20	94	83	83	12%	12%	-94	-84	-104	11%	-10%
	0.50	35	54	44	-54%	-25%	-36	-	-42	-	-17%
	1.00	18	12	-	33%	-	-17	-	-34	-	-100%

The energy dissipation capacity is calculated as the sum of area inside of each individual loop of hysteretic response. The drift of 1,0 % was taken as the reference point since it was ultimate drift for most of the specimens.

Table 5. Correlation in-between test and calculations in terms energy dissipation capacity E (kNmm^2) till d_r=1.0 %

Spec.	Test	Calc. 2nd case	Calc. 3rd case	Diff. (%)	
				2nd/test	3rd/test
I/1	6736	5534	8412	18%	-25%
I/2	7880	6738	9038	14%	-15%
I/3	6079	2014	10614	67%	-75%
I/4	10389	6644	11819	36%	-14%
III/1	4816	4602	5209	4%	-8%
III/2	12529	8115	11007	35%	12%

DISCUSSION AND CONCLUSIONS

Framed-wall models were created using the material models and finite elements that could describe their structural behaviour the best. Afterwards, they were calibrated with the test results. When concerning these results it should be noted that the properties of materials were taken as average of all specimens and also as mean values. These properties were obtained by simple tests that could not fully describe the actual situation in the structure.

Regarding the frame without infill wall specimen, the lack of bending and shear (dowel effect) stiffness for the discrete reinforcement, could lead to inappropriate model, especially in the case of dominant shear. This was compensated by increase of area of transversal reinforcement for assumed quantity.

Framed-wall models of the case 3 provided the most acceptable solution in terms of primary curves and cracks and applicability to all specimens as shown in Figs. 7., 8. and 9. The case 1 model was not able to simulate exactly the complete infill wall specimen and thus the analysis was not continued to other specimens. It was proven from this that initial values from simple tests were not sufficient. The case 2 was applicable and its accuracy was limited only to complete infill wall case. Case 3 had a user defined function for the bedjoint post-peak while others had just initial values defined.

Difficulties for case 2 and also case 3 came from inability to model the orthotropic masonry unit which was modelled as solid concrete object. Because of this, masonry units were rather pushed than crushed as it was observed in tests, due to low horizontal compressive strength (Fig.5.). In other words, model was more subdued to bejdoint sliding. This effect was not visible for complete infill wall case since the wall was framed with stronger elements. It affected the specimens with openings mostly. In Fig.5. also shown is the inclination of mortar in to holes of masonry units. This enabled for the bedjoint to hold shear till the masonry unit fails. This property was the reason for use of the post-peak function since it allowed for the shear strength to be increased for about three times with respect to initial value.

Another problem, concerning the modelling of masonry units is in inability to break due to smeared approach. The crack created in masonry unit could only lower its strength. In interaction with the interface element this had led to numerical instabilities and computational effort was implemented to find the proper post-peak curve. The concentration of stresses due to opening corners, especially windows was also one of the reasons for the poor representation of the case 2. It influenced also, but not in such quantity the results from case 3.

The stiffness values from Table 4. show that in general all models of the case 3 had somewhat lower stiffness values for the cases with openings, yet again better than compared to the case 2. Dissipated energy values from Table 5. were mostly influenced by high cycles. They showed good resemblance towards tests except for the model with eccentric door.

It can be concluded that regarding the test uncertainties, that the results of the case 3 are comparable with test results.

REFERENCES

Červenka V, Jendele L and Červenka J (2012) ATENA Program Documentation Part 1 Theory, Cervenka Consulting Ltd., Prague

Kranzler T (2008) Trägfahigkeit überwiegend horizontal beanspruchter Aussteifungsscheiben aus unbewehrtem Mauerwerk, Ph.D. Thesis, Technische Universität Darmstadt, Germany

Pryl D and Červenka J (2013) ATENA Program Documentation, Part 1 of 1, Troubleshooting Manual, Cervenka Consulting Ltd., Prague

Saneinejad A (1990) Non-linear analysis of infilled frames. Ph.D. Thesis, University of Sheffield, England

Sigmund V and Penava D (2014) "Influence of Openings, With and Without Confinement, on Cyclic Response of Infilled R-C Frames — An Experimental Study," *Journal of earthquake engineering*, 18(1):113-146

Stafford-Smith BS (1966) "Behavior of square infilled frames," *Journal of Structural Division*, 92(1):381-403